Acta Cryst. (1996). D**52**, 499–504

Refined Three-Dimensional Structure of Cat-Muscle (M1) Pyruvate Kinase at a Resolution of 2.6 Å

SIMON C. ALLEN† AND HILARY MUIRHEAD*

Department of Biochemistry and Molecular Recognition Centre, School of Medical Sciences, University of Bristol, Bristol BS8 1TD. E-mail: muirhead@bsa.bristol.ac.uk

(*Received 14 July 1995; accepted 27 November 1995*)

Abstract

The three-dimensional structure of cat-muscle pyruvate kinase has been refined at a resolution of 2.6 Å. The details of the structure permit interpretation of the original heavy-atom studies and give insight into the importance of conserved residues in pyruvate kinases and the allosteric behaviour of the enzyme. There are a small number of essential residues which determine the relative orientations of domains and the precise nature of intersubunit contacts. Arginine residues are particularly important.

1. Introduction

Pyruvate kinase (PK, E.C. 2.7.1.40) catalyses the second ATP-generating reaction of glycolysis. A phosphate group is transferred from phospho*enol*pyruvate (PEP) to adenosine diphosphate (ADP), producing pyruvate, adenosine triphosphate (ATP) and a proton. For the reaction to proceed, two bivalent metal ions are required, both usually magnesium, one bound to the ADP and the other to the enzyme. An enzyme-bound monovalent cation, usually potassium, is also required.

The enzyme is a tetramer of identical subunits, each subunit having a relative molecular mass of about 53 kDa. The amino-acid sequences of some 30 pyruvate kinases are known, from a wide variety of sources. All of these sequences have a high homology, with an identity of at least 39% (Fothergill-Gilmore & Michels, 1993). In nearly all organisms PK shows allosteric properties in binding its substrate PEP. In addition its catalytic activity is heterotropically regulated by one or more allosteric effectors, whose exact chemical nature depends on the specific organism or tissue. Thus, the residues in the effector binding site would be expected to be more variable than the conserved residues in the active site. In mammals, there are four pyruvate kinase isoenzymes: M1, found in skeletal muscle, M2, found in kidney, adipose tissue and lung, L, found in liver and R, found in erythrocytes. The M1 isoenzyme exhibits Michaelis–Menten kinetics with respect to PEP concentration and is not allosterically regulated under normal assay conditions. However, conditions have been described under which the M1 enzyme displays kinetic properties typical of a regulatory enzyme (Phillips & Ainsworth, 1977). In addition it is inhibited allosterically by high concentrations of phenylalanine at alkaline pH. This suggests that the M1 enzyme may be used as a model to consider allosteric transitions. Using the normal assay conditions the M2, L and R isoenzymes exhibit sigmoidal kinetics with respect to PEP concentration and their activity may be regulated by allosteric effectors. Additionally, the liver enzyme may be regulated by phosphorylation of a serine residue in a section of the N-terminal domain not possessed by the other isoenzymes (see Muirhead, 1987 for a review).

The molecular mechanism of allostery has been successfully investigated with a number of enzymes, where the high substrate affinity (R) state and the low substrate affinity (T) state have been elucidated by X-ray crystallographic techniques. The most notable examples are aspartate transcarbamylase (Kantrowitz & Lipscomb, 1988), glycogen phosphorylase (Johnson, Madsen, Mosley & Wilson, 1974; Fletterick, Sygusch, Murray, Madesen & Johnson, 1976; Barford & Johnson, 1989) and phosphofructokinase (Schirmer & Evans, 1990). Here, we report the refined structure of an R state pyruvate kinase; the M1 isoenzyme from cat muscle, with the future intention of using this as a basis for understanding the allosteric mechanism of pyruvate kinase. The recent determination of the structure of *Escherichia coli* pyruvate kinase in the inactive T-state (Mattevi *et al.*, 1995) has demonstrated that in the transition from the T to the R state all 12 domains of the functional tetramer modify their relative orientations while each domain retains essentially the same structure as found in the M1 R state.

2. Crystal structure and refinement

The essential three-dimensional structure of non-allosterically regulated cat-muscle (M1) pyruvate kinase was solved to a resolution of 2.6 Å by X-ray crystallographic techniques and reported by Stuart, Levine, Muirhead & Stammers (1979). The unit-cell dimensions were

† Current address: St Vincent's Institute of Medical Research, 41 Victoria Parade, Fitzroy 3065, Australia.

$a = 88.4$, $b = 115.3$, $c = 131.0$ Å, $\alpha = \beta = \gamma = 90°$. The space group of the crystal was $I222$ with one subunit in the crystallographic asymmetric unit. Thus the unit cell contains two PK tetramers each with exact 222 symmetry. In 1986, the 530-residue amino-acid sequence was determined and fitted into the structure (Muirhead *et al.*, 1986). During fitting of the sequence, the structure was refined using the program *TNT* (Tronrud, Ten Eyck & Matthews, 1987). This is the structure reported by Muirhead *et al.* (1986). Each subunit of PK (Fig. 1) comprises four domains: an N-terminal domain (residues 1–42), and domains *A* (43–115, 220–387), *B* (116–219) and *C* (388–530).

Following this, the structure was subjected to five rounds of rebuilding and refinement with *X-PLOR*, version 1.5, (Brünger, 1985) as the refinement program and three with *TNT* (Tronrud *et al.*, 1987) as the refinement program. Rebuilding the structure was accomplished with the interactive graphics program *FRODO* (Jones, 1985), running on an Evans and Sutherland 3090, using $2|F_o| - |F_c|$ and $|F_o| - |F_c|$ maps with calculated phases. Omit maps were used to assist building the less well defined regions of structure. During the course of the refinement, the *R* factor fell gradually, and the geometry of the structure improved but the refinement statistics were not wholly satisfactory and the electron-density maps were unclear for some regions of the structure, particularly for domain *B*.

At this time, the enzyme from rabbit muscle, also an M1 isoenzyme, had been crystallized and data collected to a resolution of 2.9 Å (Larsen, Laughlin, Holden, Rayment & Reed, 1994). The structure of the rabbit muscle enzyme was solved with molecular-replacement techniques, using the best cat M1 PK coordinates available at the time as the search model. The resulting rabbit muscle PK structure revealed a very similar tertiary structure to the cat PK, with the exception of two β-strands in domain *C*, at a subunit interface, and in some regions of domain *B*. The parts of the structure where differences occurred were studied and, using the rabbit muscle coordinates as a template, the cat M1 structure was rebuilt. The structure was subjected to two further rounds of rebuilding and refinement, using *X-PLOR* (Version 3.1., Brünger, 1992), with the small-molecule geometric parameters (Engh & Huber, 1991). Residues 1–11 are not seen in the electron-density maps and are presumed to be disordered. They were not included in the final rounds of refinement. The final crystallographic *R* factor is 17.5%, incorporating individually refined *B* factors. The refinement parameters are shown in Table 1. In the Ramachandran plot of main-chain dihedral angles using the program *PROCHECK* 89% of the residues are in the most favoured regions (Laskowski, MacArthur, Moss & Thornton, 1993). Thr327, which forms part of the active site and lies in a strictly conserved sequence, is the only residue in a disallowed region (Fig. 2). There are no significant differences between the refined cat-muscle structure and the rabbit-muscle structure.

Table 1. *Summary of the refinement parameters*

The R_{free} was not used in the refinement, as all the reflections were used in earlier stages of the refinement process, prior to the introduction of the R_{free}. The r.m.s. (root-mean-square) deviations are those calculated from the *X-PLOR* package, using the small-molecule geometrical parameters (Engh & Huber, 1991).

No. of non-H atoms	3976
No. of residues	519 (12–530)
No. of reflections	15440
R_{cryst} (%)	17.5 (6.0–2.6 Å, all data)
R.m.s. deviations for bond lengths (Å)	0.012
R.m.s. deviations for bond angles (°)	1.69

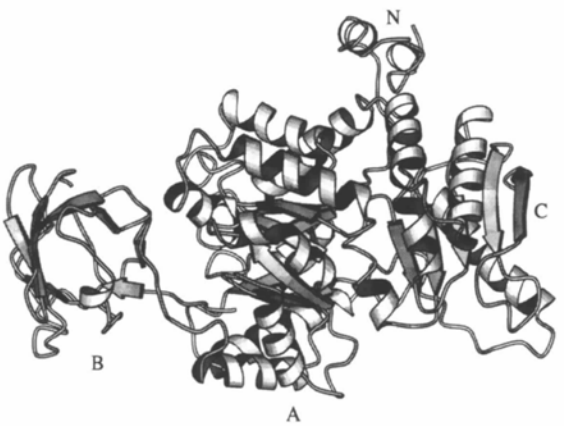

Fig. 1. A ribbon diagram of one PK subunit drawn with the program *MOLSCRIPT* (Kraulis, 1991). The N, *A*, *B* and *C* domains are indicated. The active site lies in the pocket between domains *A* and *B*. The putative effector site is between domains *A* and *C*.

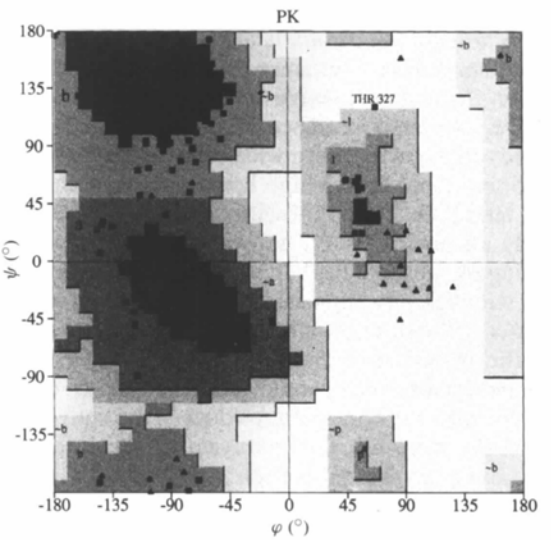

Fig. 2. Ramachandran plot of the main-chain dihedral angles. The disallowed regions are the lightest ones. Glycines are shown as triangles, the other residues as squares. Produced with *PROCHECK* (Laskowski *et al.*, 1993).

3. Structure description

The final refined structure is illustrated in Fig. 1. The monomer is shown with the domains, N *A*, *B* and *C* indicated. The representations were drawn using the program *MOLSCRIPT* (Kraulis, 1991). The elements of secondary structure are summarized in Table 2.

As assessed from the electron-density maps, the first 11 residues of the N domain have a high degree of flexibility. The secondary-structure elements in the N domain are two short helices, Nα1 and Nα2, which pack against each other. The eight-stranded α/β-barrel, domain *A*, is very well defined: the eight α-helices and the β-sheet have good hydrogen-bonding patterns. There is a continuing trend for the hydrogen bonds to be made toward the C-terminal end of the strand as the barrel progresses, demonstrating that the barrel is askew (Levine, Muirhead, Stammers & Stuart, 1978). Three short helices, following the fifth, sixth and eighth strands [Aα5(*a*), Aα6(*a*) and Aα8(*a*)] are clearly seen; similar helices are seen in triose phosphate isomerase (Banner *et al.*, 1975; Banner, Bloomer, Petsko, Phillips & Wilson, 1976). The α/β-barrel is a well known structural element and has been compared to other α/β-barrels in several previous studies (Levine *et al.*, 1978, Muirhead, 1983; Farber & Petsko, 1990). Domain *B* is composed of mainly antiparallel β-strands wound round to form a loose barrel structure; there are just a few residues that have a helical pattern, in one of the loops between the strands. Domain *C* consists of two long antiparallel helices plus a twisted five-stranded β-sheet enclosed by three helices. Strand 5 of the sheet is antiparallel to the rest. *C* domains from different subunits are related by a twofold axis of symmetry, and a continuous ten-stranded mixed β-sheet is formed across this inter-subunit boundary. The two antiparallel helices are also in this intersubunit contact forming an antiparallel helix bundle. The active site lies in the cleft between domains *A* and *B* (Muirhead *et al.*, 1986; Larsen *et al.*, 1994). It is interesting that the only residue which has dihedral angles outside the Ramachandran allowed regions – Thr327 – is a highly conserved residue which forms part of the active site and could act as the proton donor in the catalytic reaction (Larsen *et al.*, 1994). The putative effector site (Stammers & Muirhead, 1975; Stuart *et al.*, 1979) is situated between domains *A* and *C*.

The details of the refined three-dimensional structure now permit interpretation of the original heavy-atom studies (Stuart *et al.*, 1979) and also give an insight into conserved residues in pyruvate kinases and the allosteric behaviour of the enzyme.

4. Heavy-atom derivatives

Three heavy-atom derivatives were used in the initial phase determination, $KAu(CN)_2$, $K_2Pt(CN)_4$ and $GdCl_3$.

Table 2. *The secondary-structure elements in cat muscle M1 pyruvate kinase*

The secondary structure ws assessed using the program *DSSP* (Kabsch & Sander, 1983).

Residue numbers	Secondary-structure element
Leu17–Ala20	Nα1
Phe25–Cys30	Nα2
Gly45–Thr49	*A*β1
Val57–Lys65	*A*α1
Met68–Asn74	*A*β2
His80–Glu95	*A*α2
Ala108–Asp112	*A*β3
Ile118–Thr120	*B*β1
Glu132–Leu133	*B*β2
Thr138–Thr142	*B*β3
Val155–Trp157	*B*β4
Ile163–Val166	*B*α1
Lys172–Val175	*B*β5
Ile180–Lys187	*B*β6
Phe191–Val196	*B*β7
Gly200–Ser201	*B*β8
Gly207–Asn209	*B*β9
Glu222–Glu233	*A*α3
Met238–Ala241	*A*β4
Ala247–Leu257	*A*α4
Lys265–Ile270	*A*β5
Glu274–Arg278	*A*α5(*a*)
Phe279–Ala285	*A*α5
Gly288–Ala292	*A*β6
Arg293–Glu299	*A*α6(*a*)
Val305–Ala319	*A*α6
Val323–Ala326	*A*β7
Arg341–Asp353	*A*α7
Cys357–Leu360	*A*β8
Gly362–Ala365	*A*α8(*a*)
Pro370–Ala386	*A*α8
His390–Ser401	*C*α1
Leu407–Cys422	*C*α2
Leu427–Leu430	*C*β1
Arg435–Arg442	*C*α3
Ile449–Thr453	*C*β2
His456–Gln461	*C*α4
Ile468–Val472	*C*β3
Trp481–Ala498	*C*α5
Val507–Thr512	*C*β4
Thr523–Pro528	*C*β5

Attempts to label reactive sulfydryl groups with mercurials either led to loss of crystallinity or produced very large intensity changes (Stammers & Muirhead, 1975). Upon examination of the refined structure, this is not surprising, since there are nine cysteine residues per subunit, some of which are deeply buried in the interior of the molecule. However, the gold derivative, potassium aurocyanide, binds to three independent sites. The first site is 2.8 Å from the SG of Cys30 at the end of helix Nα2, while the second is 2.0 Å from the SG of Cys473 at the end of the β-strand Cβ3. The third site is 2.5 Å from the NH1 of Arg525. In all three cases a covalent interaction could be present and other side chains provide a relatively hydrophobic environment for the $[Au(CN)_2]^-$ moiety.

The platinum derivative, $K_2Pt(CN)_4$, caused a change in space group from $I222$ to $P2_122_1$, unless the crystals were pre-soaked in glutaraldehyde. The change in space group corresponds to a loss of two crystallographic twofold axes parallel to the x and z crystal axes, respectively. Two independent heavy-atom binding sites were observed with this derivative. One platinum site is 3.6 Å from the NZ of the highly reactive Lys366 at the entrance to the active site. The second site is 2.8 Å from the NE1 of Trp514 in the loop connecting the two antiparallel beta strands Cβ4 and Cβ5. This site is at a subunit interface related by the y crystallographic axis, explaining the loss of crystallographic symmetry in the absence of glutaraldehyde.

The platinum and gold derivatives were obtained at pH 6. A third derivative was obtained by changing the pH to 8 and soaking the crystals in $GdCl_3$. The gadolinium ion binds at the same position as the enzyme bound bivalent cation which is essential for activity. It is 2.8 Å from the OE1 of Glu271 and 3.1 Å from the OD2 of Asp295. Both residues are strictly conserved.

The residues involved in heavy-atom binding are shown in Table 3.

Table 3. *The heavy-atom binding sites in PK and their structural features*

Site	Adjacent residues	Structural features
Au(1)	SG of Cys30, O of Leu26, Leu26 side chain, Arg318 side chain	C-terminus of Nα2 hydropohobic environment *A*α6 of *Z*-related subunit
Au(2)	SG of Cys473, OD of Asp475, Leu487 and Leu491	C-terminus of *C*β3, near surface of tetramer hydrophobic environment
Au(3)	Guanidinium group of Arg525 Near Val489, Met493, Val510, Val527.	Near *Y*-axis interface Hydrophobic pocket formed By *C*α5, *C*β4 and *C*β5
Pt(1)	OD of Asn74, NZ of Lys366, His77 & Thr49	C-terminus of *A*β2, loop connecting *A*β8 and *A*α8 in vicinity
Pt(2)	Trp514, Arg515, Ser518, Asn522. Arg525, Val527	*C*β4/*C*β5 Side chains close by *C*β5 of symmetry-related subunit (*y*-axis).
Gd	OE of Glu271, OD of Asp295	C-terminus of *A*β5, C-terminus of *A*β6

5. Allostery

The active site of PK lies in a deep cleft between domains *A* and *B* and the residues involved in binding and catalytic activity are totally conserved in all PK amino-acid sequences. There are two pockets between domains *A* and *C* separated by the flexible connection between domain N and *A*β1 of domain *A* and the relatively rigid connection between *A*α8 of domain *A* and *C*α1 of domain *C*. The putative effector site consists of one of these pockets and it has been proposed that this pocket is open in the R quaternary structure and closed in the T structure (Walker, Chia & Muirhead, 1992; Muirhead & Watson, 1992). Residues in this pocket do not show the same degree of conservation as those in the active site; this is consistent with the fact that different PK's use a variety of allosteric effectors.

There are two major intersubunit contacts. The contact between the two subunits related by the crystallographic y axis (the *Y* contact) involves domains N and *C* (Fig. 1). The contact between the two subunits related by the z crystallographic axis (the *Z* contact) involves all four domains and includes residues close to the active site. A study of the binding of the allosteric effector fructose bisphosphate to yeast PK (Murcott, Gutfreund & Muirhead, 1992) led to the suggestion that the tetramer is a dimer of dimers with relatively small differences between the R and T quaternary structures in the *Z* contact and larger differences in the *Y* contact. The *Y* contact involves rigid elements of secondary structure; namely two α-helices (*C*α1 and *C*α2) and a β-strand (*C*β5) in each subunit so that only discrete modes of packing are possible. This contact is illustrated in Fig. 3.

The part of the extensive *Z* interface which is close to the active site involves domain *B* and several connecting loops in domain *A* which could give rise to a variety of closely connected structures.

The differences between the M1 and M2 isoenzymes emphasise the importance of the *Y* interface. These isoenzymes are different only in one region, coded for by a single exon, the different isoenzymes being formed by different splicing of the mRNA (Noguchi, Inoue & Tanaka, 1986). In terms of this structure, these residues are to be found mainly at the *C* domain/*C* domain

Fig. 3. Domain *C* of two cat pyruvate kinase M1 monomers, illustrating the *Y* contact in the tetramer. The secondary-structure elements most deeply involved in the intersubunit contact, *C*α1, *C*α2 and *C*β5 are indicated. *C*β1, which together with *C*α1 and *C*α2, contains the residues that differ between the M1 and M2 isoenzymes is also labelled. Note that the β-strands from a continuous antiparallel sheet across the subunit interface.

interface, *viz* $C\alpha1$, $C\alpha2$, $C\beta1$ and the loops between them. Since under normal physiological and assay conditions only the M2 enzyme is allosterically regulated, not the M1, this region must be critical for conferring a structural transition from a high substrate affinity (R) state to a low substrate affinity (T) state.

A reasonable hypothesis (Walker *et al.*, 1992) is that when the allosteric activator binds to the T structure the effector pocket is opened and the second A/C pocket closes. This alters the relative orientations of domains *A* and *C* and destabilizes the packing at the *Y* interface in favour of the R quaternary structure. This change in quaternary structure due to the change in packing of the *C* domains affects packing at the *Z* interface, leads to a change in the relative orientations of domains *A* and *B* and hence increases the affinity for substrate at the active site. There are very few totally conserved residues in domains N, *B* and *C*. However, the design and expression of a mutant of yeast PK (Ser384 to Pro, in the middle of $C\alpha2$) confirmed the importance of the *Y* interface, since the mutant was essentially locked in the T state (Collins, McNally, Fothergill-Gilmore & Muirhead, 1995). Mutations in the A/C domain interface have shown that this region also influences the R/T equilibrium (Walker *et al.*, 1992).

6. Conserved residues

The conserved residues at the domain interfaces and subunit interfaces are shown in Table 4(*a*)–(*c*).

Conserved residues in the wide range of known sequences should tell us something about the regulation of PK as well as its catalytic activity. We would not expect to find conserved residues in the *Y* interface – the packing there is more a function of the secondary structure. More surprisingly there are only two conserved residues in the A/C interdomain contact. Asp356, which is at the beginning of strand $A\beta8$, is totally conserved and Arg444 is conserved except in *Escherichia coli*. In the M1 crystal structure there is a salt bridge between the carboxyl group of the conserved Asp356 in domain *A* and the guanidinium group of the arginine in domain *C*. In *E. coli* the nearby Arg441 could play an equivalent role. This salt bridge would help to defined the relative orientations of domains *A* and *C*. It is linked to the structure of the effector binding site *via* the hydrogen bonds linking strands $A\beta1$ and $A\beta8$ of the α/β-barrel of domain *A* (the carbonyl of Asp356 bonded to the amide of Gly45). A *Trypanosoma bruceii* mutant in which Arg45 is replaced by glycine demonstrates that this residue is involved in binding the allosteric effector (Ernest, Callens, Muirhead, Opperdoes & Michels, unpublished work).

The stretch of polypeptide leading from domain *A* to domain *B* (residues 111–119) is highly conserved. In particular the interactions of the side chain of Arg119 with Glu117 (interdomain link), Ser76 and His77 (loop connecting $A\beta2$ to $A\alpha3$) would help to determine the relative orientation of domains *A* and *B* and hence the configuration of the active-site residues. This is confirmed by the existence of a mutant human PK in which Arg119 is replaced by a cysteine. This mutant displays negative cooperativity and a high affinity for PEP (Neubauer *et al.*, 1991). One other conserved residue in domain *B* is Asn209 which interacts with Glu299 on a conserved loop, $A\beta6/A\alpha6$ in domain *A*.

The conserved residues at the *Z* axis interface involve interactions between domain *A* and the symmetry-related domain *A*; the domain *B* and the symmetry-related domain *A*. Asp177 forms part of the close contact of one subunit with Arg341 of the *Z* axis-related subunit. This is the only conserved region in domain *B* apart from the residues 111–119 connecting domains *A* and *B*. In

Table 4. *Conserved residues at domain and subunit interfaces*

All numbering is using the cat M1 isoenzyme. All sequences are in the SWISS-PROT (Bairoch & Boeckmann, 1994) database or cited in Fothergill-Gilmore & Michels (1993). The tertiary and quaternary structures are stabilized by salt bridges between domains *A* and *B* and between domains *A* and *C* together with interactions across the *Z* interface.

(*a*) Conserved residues at the domain *A*/domain *B* interface

Conserved residue and location	Interaction of residue across interface
Ser76 ($A\beta2/A\alpha2$)	CO hydrogen bonded to Arg119
His77 ($A\beta2/A\alpha2$)	Side chain close to guanidinium group of Arg119
Glu117 (not present in *E. coli* type 2) (*A*/*B* connecting link)	Close to active site. Salt link to Arg119
Arg119 (domain *B*, $B\beta1$)	Interacts with carboxyl group of Glu117, carbonyl of residue 76 and imidazole of His77
Asn209 ($B\beta9$)	Glu299 and Asp295
Asp295 [$A\alpha6(a)$]	Asn209
Glu299 [$A\alpha6(a)$]	Asn209

(*b*) Conserved residues at the domain *A*/domain *C* interface

Conserved residue and location	Interaction of residue across interface
Asp356 ($A\alpha7/A\beta8$)	Side chain forms salt bridge to Arg444, carbonyl hydrogen bonded to amide of residue 45 in $A\beta1$
Arg444 ($C\alpha3/C\beta2$, not present in *E. coli* types 1 and 2)	Interacts with Asp356 and carbonyl of Gly354
Pro445 ($C\alpha3/C\beta2$, not present in *E. coli* type 2)	Stabilizes immediate environment of Arg444

(*c*) Conserved residues at the *Z* intersubunit contact

Conserved residue and location	Interaction of residue across the 'z' axis to residue in symmetry-related subunit
Asp177 ($B\beta5/B\beta6$)	Arg341
Gly178 ($B\beta5/B\beta6$)	Holds Asp1776 in position. Position 3 of β-bend
Gly297 [$A\alpha6(a)$]	Close contact with *z*-related subunit
Gln328 ($A\beta7/A\alpha7$)	Arg341
Ser332 ($A\beta7/A\alpha7$)	Glu343 ($A\alpha7$)
Arg341 ($A\alpha7$)	Large number of close interactions

general the conserved loops in domain *A*, which form part of the active site and also interact with Arg341, comprise residues 326–333 ($A\beta7/A\alpha7$) and residues 359–363 ($A\beta8/A\alpha8$).

Thus, the tertiary and quaternary structures in the R state are stabilized by salt bridges between domains *A* and *B* and between domains *A* and *C* together with interactions across the *Z* interface. There are a small number of essential residues which determine the relative orientations of domains and the precise nature of intersubunit contacts. Arginine residues are particularly important in defining these salt bridges. The interactions across the *Y* interface are determined by the packing of elements of regular secondary structure and are less influenced by the precise nature of the side chains.

The atomic coordinates have been deposited with the Brookhaven Protein Data Bank.*

We are grateful to Dianne Walker, Toby Murcott and Linda Fothergill-Gilmore for useful discussions and to the SERC for funding.

* Atomic coordinates and structure factors have been deposited with the Protein Data Bank, Brookhaven National Laboratory (Reference: 1PKM R1PKMSF). Free copies may be obtained through The Managing Editor, International Union of Crystallography, 5 Abbey Square, Chester CH1 2HU, England (Reference: AD0012).

References

Bairoch, A. & Boeckmann, B. (1994). *Nucleic Acid Res.* **22**, 3578–3580.

Banner, D. W., Bloomer, A. C., Petsko, G. A., Phillips, D. C., Pogson, C. I. & Wilson, I. A. (1975). *Nature (London)*, **255**, 609–614.

Banner, D. W., Bloomer, A. C., Petsko, G. A., Phillips, D. C. & Wilson, I. A. (1976). *Biophys. Res. Commun.* **72**, 146–155.

Barford, D. & Johnson, L. N. (1989). *Nature (London)*, **340**, 609–616.

Brünger, A. T. (1985). *X-PLOR Manual, Version 1.5*, Yale University, New Haven, Connecticut, USA.

Brünger, A. T. (1992). *X-PLOR Manual, Version 3.1*, Yale University, New Haven, Connecticut, USA.

Collins, R. A., McNally, T., Fothergill-Gilmore, L. A. & Muirhead, H. (1995). *Biochem. J.* **310**, 117–123.

Engh, R. A. & Huber, R. (1991). *Acta Cryst.* A**47**, 392–400.

Farber, G. K. & Petsko, G. A. (1990). *Trends Biochem Sci.* **15**, 228–234.

Fletterick, R. J., Sygusch, J., Murray, N., Madsen, N. B. & Johnson, L. N. (1976). *J. Mol. Biol.* **103**, 1–17.

Fothergill-Gilmore, L. A. & Michels, P. A. M. (1993). *Prog. Biophys. Mol. Biol.* **59**, 105–235.

Johnson, L. N., Madsen, N. B., Mosley, J. & Wilson, K. (1974). *J. Mol. Biol.* **90**, 703–717.

Jones, T. A. (1985). *Methods Enzymol.* **115**, 157–171.

Kabsch, W. & Sander, C. (1983). *Biopolymers*, **22**, 2577-2635.

Kantrowitz, E. R. & Lipscomb, W. N. (1988). *Science*, **241**, 669–674.

Kraulis, P. J. (1991). *J Appl. Cryst.* **24**, 946–950.

Larsen, T. M., Laughlin, L. T., Holden, H. M., Rayment, I. & Reed, G. H. (1994). *Biochemistry*, **33**, 6301–6309.

Laskowski, R. A., MacArthur, M. W., Moss, D. S. & Thornton, J. M. (1993). *J. Appl. Cryst.* **26**, 283–291.

Levine, M., Muirhead, H., Stammers, D. K. & Stuart, D. I. (1978). *Nature (London)*, **271**, 626–630.

Mattevi, A., Velentini, G., Rizzi, M., Speranza, M. L., Bolognesi, M. & Coda, A. (1995). *Structure*, **3**, 729–741.

Muirhead, H. (1983). *Trends Biochem. Sci.* **8**, 326–329.

Muirhead, H. (1987). *Pyruvate Kinase*, in *Biological Macromolecules and Assemblies*, edited by F. A. Jurnak and A. McPherson, Vol. 3, pp. 143–186. New York: John Wiley.

Muirhead, H., Clayden, D. A., Barford, D., Lorimer, C. G., Fothergill-Gilmore, L., Schiltz, E. & Schmitt, W. (1986). *EMBO J.* **5**, 475–481.

Muirhead, H. & Watson, H. (1992). *Curr. Opin. Struct. Biol.* **2**, 870–876.

Murcott, T. H. L., Gutfreund, H. & Muirhead, H. (1992). *EMBO J.*, **11**, 3811–3814.

Neubauer, M., Lakomek, M., Winkler, M., Parke, S., Hofferbert, S. & Schrter, W. (1991). *Blood*, **77**, 1871–1875.

Noguchi, T., Inoue, H. & Tanaka, T. (1986). *J. Biol. Chem.* **261**, 13807–13812.

Phillips, F. C. & Ainsworth, S. (1977). *Int. J. Biochem.* **8**, 729–738.

Schirmer, T. & Evans, P. R. (1990). *Nature (London)*, **343**, 140–145.

Stammers, D. K. & Muirhead, H. (1975). *J. Mol. Biol.* **95**, 213–225.

Stuart, D. I., Levine, M., Muirhead, H. & Stammers, D. K. (1979). *J. Mol. Biol.* **134**, 109–142.

Tronrud, D. E., Ten Eyck, L. F. & Matthews, B. W. (1987). *Acta Cryst.* A**43**, 489–500.

Walker, D., Chia, W. N. & Muirhead, H. (1992). *J. Mol. Biol.* **228**, 265–276.